CONF-941144--117

DETERMINATION OF SITE-OCCUPANCIES IN ALUMINIDE INTERMETALLICS BY ALCHEMI

I.M. ANDERSON*, A.J. DUNCAN†, AND J. BENTLEY*
*Oak Ridge National Laboratory, Metals and Ceramics Division, P.O. Box 2008, MS-6376, Oak Ridge, TN 37831-6376; †University of Florida, Department of Materials Science and Engineering, Gainesville, FL 32611

ABSTRACT

The site-distributions of Fe in four B2-ordered NiAl-based alloys with Fe concentrations of 10%, 2%, and 0.5% have been determined by ALCHEMI (atom-location by channeling-enhanced microanalysis). Site-distributions have been extracted with standard errors between ~1.5% (10% Fe concentration) and ~6% (0.5% Fe concentration). The results show that Fe has no strong site-preference in NiAl and tends to reside on the site of the stoichiometrically deficient host element.

An improved ALCHEMI analysis procedure is outlined. The analysis explicitly addresses the phenomenon of ionization delocalization, which previously complicated the determination of site-distributions in aluminide intermetallics, leading to inaccurate and oftentimes nonphysical results. The improved ALCHEMI analysis also addresses the presence of anti-site defects. The data acquisition conditions have been optimized to minimize the sources of statistical and systematic error. This optimized procedure should be suitable for all analyses of B2-ordered alloys. Several analyses at different channeling orientations show that the extracted site-occupancies are robust as long as the data are acquired at orientations that are remote from any major pole of the crystal.

INTRODUCTION

The site-distributions of alloying additions in ordered intermetallic alloys are among the basic chemical characteristics of the material, which together with stoichiometry, grain structure, phase distribution, etc., determine the properties of the alloy. The mechanical properties of ordered alloys can be modified by introducing minor amounts of an alloying addition that resides on one of the regular lattice sites of the crystal.[1] Proper modeling and understanding of such property changes depends upon an accurate knowledge of the site-occupancies.

The site-distributions of alloying additions in aluminide intermetallics can now be extracted reliably by the ALCHEMI technique, as a result of recent improvements.[2,3] ALCHEMI held initial promise for the extraction of site-distributions[4] but was plagued by a complication, ionization delocalization,[5] that rendered the extracted site-distributions inaccurate and sometimes nonphysical.[6,7] This complication is especially pronounced for alloys such as aluminides and silicides that contain light elements. For example, consider ALCHEMI analyses of an $L1_2$-ordered $Ni_{76}Al_{21}Hf_3$ alloy. Conventional ALCHEMI analysis predicted that the fraction of Hf on the 'Al'-site, $p_{Hf'Al'}$, was -127%;[6] reanalysis of the same specimen by statistical ALCHEMI[8] gave $p_{Hf'Al'} = -220\pm190\%$.[9] Analysis of the same data set with our revised ALCHEMI analysis,[3] which explicitly addresses ionization delocalization, indicates that $p_{Hf'Al'} = 80\pm25\%$. Reduction of the large standard error of this result should result if the data acquisition parameters were optimized. However, this qualitative result is reasonable and consistent with atom probe field ion microscopy (APFIM) studies of similar alloys of stoichiometry $Ni_{76}Al_{24-x}Hf_x$, for which $p_{Hf'Al'}$ was 76.9±8.3% (x = 0.5) and 84.4±3.5% (x = 1).[10]

ALCHEMI is performed by acquiring energy-dispersive X-ray (EDX) spectra from a single region of a specimen at a variety of diffracting conditions. Conventional EDX spectrometry is performed at a weakly diffracting orientation of the crystal and ideally all sites in the unit cell experience the same depth-averaged electron intensity. For ALCHEMI, a crystal is probed at a series of orientations with the incident electron beam oriented near a high-symmetry orientation of the crystal, indicated by a pole or a Kikuchi band in the diffraction pattern, where slight changes in specimen-orientation can result in large changes in the depth-averaged electron intensities at the various sites of the crystal. In the vicinity of a Kikuchi band, all diffracting conditions between a weakly diffracting orientation and the strongly diffracting symmetry orientation are sampled

within a few degrees of specimen tilt, as depicted schematically for NiAl in Fig. 1a. Here, the gray levels of the atoms on the two sites represent the corresponding incident electron intensities. The characteristic X-ray signal from the atoms on these sites varies proportionately to the incident electron intensity; Fig. 1b shows data acquired near a {200} Kikuchi band of NiAl. The coordinates r_i are the characteristic X-ray intensities relative to those acquired at a weakly channeling orientation of the crystal, as defined below. Approaching the Kikuchi band from the weakly diffracting reference orientation, the characteristic X-ray intensities of both host elements initially decrease; the aluminum intensity then rises rapidly as the orientation of the crystal passes through the first-order Bragg condition; then the nickel intensity rises, while the aluminum intensity falls, as the crystal is tilted toward the symmetry orientation. This sequence of diffracting conditions gives good discrimination between the sites of the crystal. The site-occupancies of the alloying additions distributed throughout the crystal are determined by correlating the variation of their characteristic X-ray intensities at different diffracting conditions with those of the host elements, which are used as marker elements for the sites of the crystal.

The strengths and limitations of ALCHEMI follow from the physical basis underlying the technique. Because site-distributions are determined by correlating characteristic X-ray intensities, data interpretation and analysis are relatively uncomplicated. However, the simplicity of the analysis imposes limitations: there is no way to assess whether the host elements reside only on their respective sublattices; interstitial site-occupancies are beyond the scope of the technique; and point-defect concentrations can be inferred only indirectly from the determined site-occupancies. ALCHEMI is spectroscopic and distinguishes unambiguously between neighboring elements in the periodic table. Another advantage of ALCHEMI relative to APFIM or resonant anomalous X-ray scattering (RAXS) is that ALCHEMI requires only a simple analytical electron microscope (AEM) and is thus economical and widely available. In addition, the diffraction and imaging capability of the AEM allows complementary characterization of the microstructure and careful selection of the analyzed area and experimental conditions.

Our revised ALCHEMI analysis procedure[3] can be summarized as follows:

- a number of spectra are acquired from a single area of the specimen at different crystal orientations, including a weakly diffracting reference orientation;
- the intensities $I_i^{(\xi)}$ of the characteristic X-rays of the elements i of interest that are extracted from each spectrum ξ are divided by the corresponding intensity at the reference orientation (0) yielding intensity ratios, $r_i^{(\xi)} = I_i^{(\xi)} / I_i^{(0)}$;

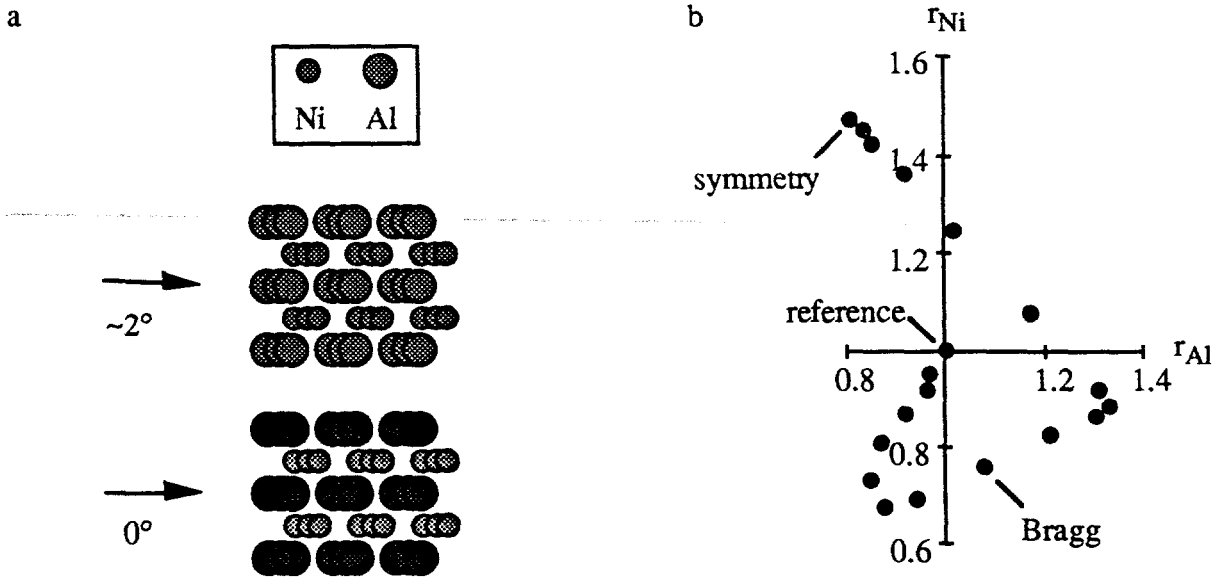

Fig. 1. The physical basis for ALCHEMI. See text for details. (a) Schematic representation of the variation of the depth-averaged electron intensity on the two sublattices of B2-ordered NiAl. (b) Relative variation in the characteristic intensities of the host elements. Selected diffracting conditions are indicated.

- the intensity ratio of each alloying element (k) is fit to the intensity ratios of the marker elements (j = 1, ..., n):

$$r_k^{(\xi)} = \alpha_{k0} + \alpha_{k1} r_1^{(\xi)} + \ldots + \alpha_{kn} r_n^{(\xi)} \; ; \qquad (1)$$

  best-fit values and uncertainties are obtained for the correlation coefficients, α_{kj};
- if there is no ionization-delocalization or anti-site occupancies, the site occupancies are $p_{kj} = \alpha_{kj}$; otherwise the correlation coefficients can be corrected for ionization delocalization and the site-occupancies of the alloying additions can be calculated if the anti-site distribution is known or can be assumed.

A worked example is presented in the next section as an illustration of our revised ALCHEMI analysis. The succeeding section reports site-distributions of Fe in four B2-ordered NiAl-based alloys, which have been analyzed under identical experimental conditions. Also, the results of ALCHEMI analyses of one alloy at a number of distinct channeling orientations are reported and various factors that bear on the reliability of the procedure are discussed.

A Worked Example

A thin foil specimen of an alloy of composition $Ni_{50}Al_{40}Fe_{10}$ was examined in a Philips CM12 AEM equipped with a LaB_6 filament and operated at 120 kV. X-rays were detected with an EDAX lithium-drifted silicon detector with a super-ultra-thin-window and analyzed with an EDAX 9900 EDX spectrometer. Experiments were performed with a beam divergence semi-angle of one quarter of the Bragg angle, $\theta_B \approx 12$ mrad, of a fundamental 200 reflection. Eighteen spectra were acquired including a weakly diffracting reference spectrum. Four of these spectra are shown in Figure 2, all at the same scale. The count rates of the Ni-K_α, Al-K_α, and Fe-K_α peaks, $(I_{Ni}^{(\xi)}, I_{Al}^{(\xi)}, I_{Fe}^{(\xi)})$, were extracted from each spectrum, ξ:

{(616, 318, 127), (478, 285, 101), (622, 456, 181), (955, 290, 130), ...} .

(a) reference orientation
$\mathbf{r} = (1, 1, 1)$

(b) $\theta / \theta_B = 1.25$
$\mathbf{r} = (0.77, 0.89, 0.80)$

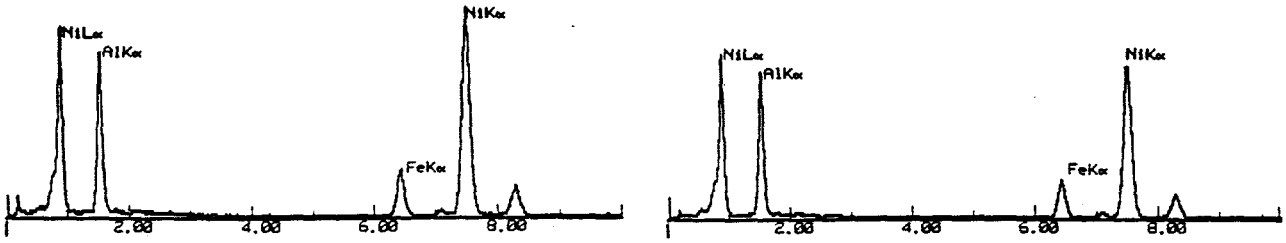

(c) $\theta / \theta_B = 0.9$
$\mathbf{r} = (1.01, 1.43, 1.43)$

(d) $\theta / \theta_B = 0$ (symmetry)
$\mathbf{r} = (1.55, 0.91, 1.02)$

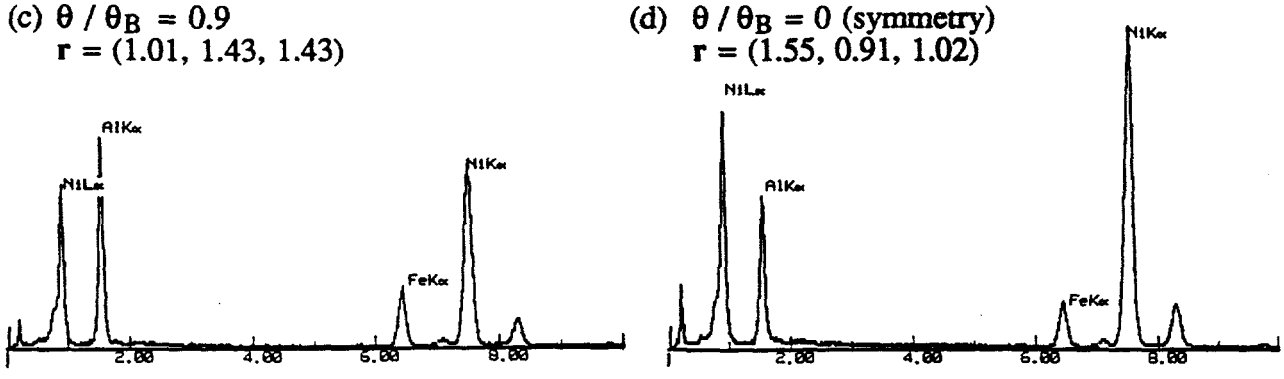

Fig. 2. EDX spectra, diffracting conditions, and characteristic X-ray intensity ratios $\mathbf{r} = (r_{Ni}, r_{Al}, r_{Fe})$ for four specimen orientations.

The elemental count rates in each spectrum were then divided by the corresponding elemental count rate of the reference spectrum to obtain $\mathbf{r}^{(\xi)} = (r_{Ni}^{(\xi)}, r_{Al}^{(\xi)}, r_{Fe}^{(\xi)})$ values:

$$\{(1, 1, 1),\ (0.77, 0.89, 0.80),\ (1.01, 1.43, 1.43),\ (1.55, 0.91, 1.02),\ \ldots\}\ .$$

The value of $r_i^{(0)}$ is 1 by definition; the value of $r_i^{(\xi)}$ yields the orientation effect for element i and spectrum ξ. The r-data are fit to a plane, which has the equation:

$$r_{Fe}^{(\xi)} = \alpha_{Fe0} + \alpha_{FeNi}\, r_{Ni}^{(\xi)} + \alpha_{FeAl}\, r_{Al}^{(\xi)}\ . \qquad (1a)$$

Figure 3 shows plots of this data set (a) in the best-fit plane of the data and (b) looking down onto the best-fit plane. The correlation coefficients, α_{kj}, are:

$$\alpha_{FeNi} = 0.262 \pm 0.015\ ; \quad \alpha_{FeAl} = 1.048 \pm 0.022\ . \qquad (2)$$

Ionization of the K-shells of Fe and Ni is almost entirely localized and the concentration of $Ni_{'Al'}$ anti-site defects should be small; hence we expect that $p_{Fe'Ni'} \approx \alpha_{FeNi}$. Conversely, the ionization of the Al K-shell is highly delocalized; hence the correlation coefficient α_{FeAl} requires a significant delocalization correction. The correction procedures for ionization delocalization and anti-site defects are too involved to be included here, but such corrections to the α_{kj} yield:[3]

$$p_{Fe'Ni'} = 0.253 \pm 0.015\ ; \quad p_{Fe'Al'} = 0.762 \pm 0.017\ . \qquad (3)$$

The sum of the two site-occupancies is equal to one to within the statistical uncertainty of the measurement. These site-distributions were calculated assuming that $Ni_{'Al'}$ anti-site defects and not vacant 'Al'-sites ($V_{'Al'}$) are the predominant constitutional point-defects.[11] Consistent with this assumption, the anti-site concentration is:

$$p_{Ni'Al'} = 0.051 \pm 0.003\ , \qquad (4)$$

that is, ~5% of the Ni atoms occupy 'Al'-sites.

Results and Discussion

The site-distributions of four different B2-ordered alloys of Fe-doped NiAl were analyzed under the same experimental conditions as those of the worked example in the previous section. Table I summarized the compositions, heat treatments, extracted site-distributions, and inferred

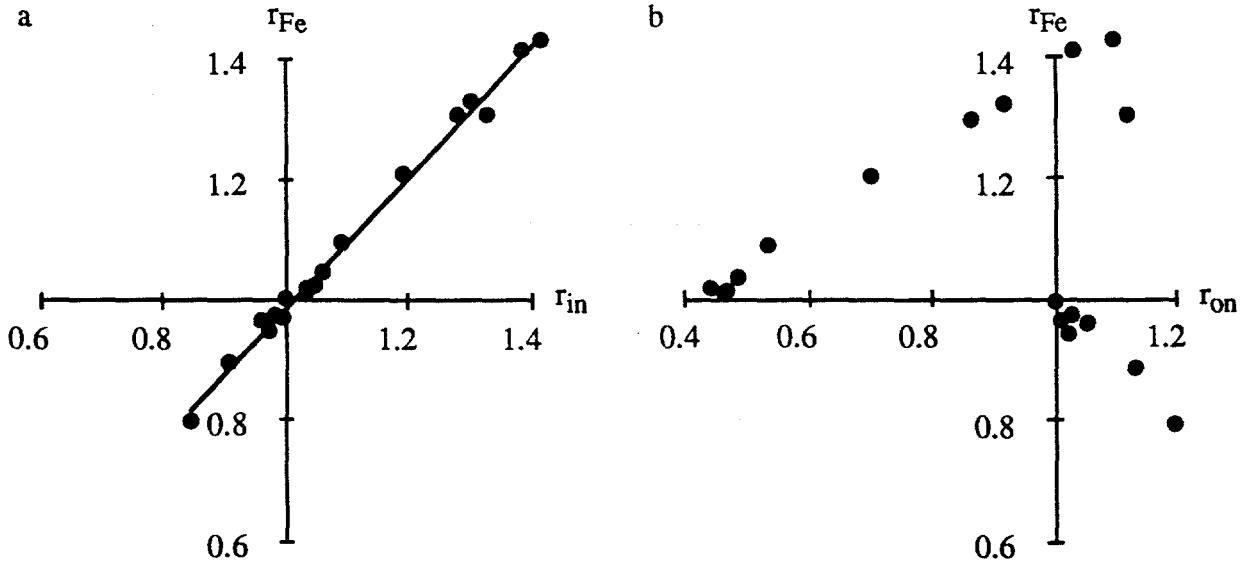

Fig. 3. Two-dimensional projections of a three-dimensional ALCHEMI data set showing (a) the scatter of the data out of the best-fit plane and (b) the spread of the data across the best-fit plane. The abscissae r_{in} and r_{on} are orthonormal linear combinations of the coordinates r_{Ni} and r_{Al}.

Table I. Site-occupancies of Fe and inferred point-defect concentrations in NiAl-based alloys.

Alloy composition (at.%)			Heat Treatment	Site-occupancy	Point-defects	
Ni	Al	Fe		$p_{Fe'Ni'}$	Type	% of sites
50	40	10	#1	25.3 ± 1.5	$Ni'_{Al'}$:	5.1 ± 0.3
40	50	10	#1	88.0 ± 1.8	$V_{Ni'}$:	4.7 ± 0.7
47.3	50.7	2	#2	94.1 ± 3.2	$V_{Ni'}$:	3.2 ± 0.2
49.75	49.75	0.5	#1	54.5 ± 6.2	$Ni'_{Al'}$:	0.0 ± 0.1

#1: 1300°C (5 h) + 800°C (12 h)

#2: 1000°C (1 h) + extrude 9:1 + 900°C (1 h) + 800°C (1 h)

point-defect concentrations of the four alloys. These results show that Fe tends to reside on the site of the stoichiometrically deficient host element, but that a fraction resides on the alternative site, suggesting that Fe is accommodated onto both sites in NiAl with no significant site preference. The inferred constitutional point-defect concentrations for both alloys containing 10% Fe are ~5%. The standard errors of the site-distributions scale as one over the square-root of the Fe concentration, reflecting the $1 / \sqrt{N}$ relative uncertainty of the Poisson counting statistics.

The results in Table I were acquired under experimental conditions that have been tested and optimized to minimize the sources of statistical and systematic error in the analysis. A great deal of effort has gone into selecting these "standard" conditions. The orientation of the specimen was carefully chosen. It has been determined that although a larger variation in the characteristic X-ray intensities is observed with axial channeling conditions (e.g., at <001>), better statistical confidence is achieved with {200} channeling conditions because the planar channeling gives greater discrimination between the two sites. Extreme care was taken to avoid nonsystematic reflections during data acquisition so that the channeling variation would result only from the 200 systematic row. The position along the 200 Kikuchi band was chosen to be remote from any major poles: ~14° from the dominant <001> pole and ~4.4° from <013>. This orientation should be appropriate for all analyses of B2-ordered alloys.

Additional experiments were performed on the specimen of composition $Ni_{50}Al_{40}Fe_{10}$ in order to test the robustness of the results obtained with this procedure. These results are summarized in Table II. The results of four ALCHEMI experiments performed ~4° or further from a major pole yield similar results. The [unweighted] average of the four site-distributions determined at these experimental conditions is $p_{Fe'Ni'} = 25.3 \pm 1.2\%$: the spread of these values is consistent with random normal statistical variation as reflected by the experimentally measured standard error. Conversely, the site-distributions determined from ALCHEMI experiments performed ~3° or less from a major pole are significantly different from the other values: if either of these two outlying points are included in the average, the standard deviation increases to at least ±2.0, which is greater than the standard error of any of the individual measurements and inconsistent with a random normal statistical variation. These results suggest that the site-distributions determined by this method are robust as long as the data are acquired at a position on the Kikuchi band that is remote from any major poles. This criterion is not entirely subjective. The diffraction pattern is a reliable guide for assessing the importance of adjacent poles during data acquisition. For the two outlying data sets in Table II, the <013> pole is prominent in many of the diffraction patterns. Moreover, the "shape" of the intensity variation shown in Fig. 1b should be similar as long as only the systematic reflections contribute to the channeling variation; this shape-invariance is obeyed by the four data sets in Table II that yield similar site-distributions; in contrast, the shape of the intensity variations for the data set acquired nearest <013> is different. Finally, the sum of the correlation coefficients after delocalization correction (and of the independent site-distributions, e.g., in equation (3)) should be one. For the two outlying results, the sum of the coefficients differs from one by >1.5 standard errors.

Table II. Site-occupancies of Fe in $Ni_{50}Al_{40}Fe_{10}$ for data acquired at a variety of orientations.

Orientation relative to		Orientation relative to		Site-occupancy
<001>	<011>	nearest major pole		$p_{Fe'Ni'}$
11.3°	33.7°	7.1°	<013>	26.6 ± 1.4 *
14.0°	31.0°	4.4°	<013>	25.3 ± 1.5 *
				23.7 ± 1.3 *
16.1°	28.9°	2.3°	<013>	32.0 ± 2.4
21.4°	23.6°	3.0°	<013>	29.0 ± 1.7
30.5°	14.5°	3.9°	<012>	25.6 ± 1.6 *

* These results are consistent with a random normal statistical distribution.

CONCLUSIONS

ALCHEMI has become a reliable technique for the extraction of the site-distributions of alloying additions in aluminide intermetallics. Our improved formulation of ALCHEMI analysis explicitly addresses ionization delocalization and thus overcomes the major complication of earlier formulations of ALCHEMI, which rendered the extracted site-distribution from aluminides inaccurate and sometimes nonphysical. The experimental conditions for the analysis of B2-ordered alloys have been optimized. This optimized analysis method has been applied to determine the site-distributions of Fe in four B2-ordered NiAl-based alloys. Quantitative site-distributions have been determined with a standard error of ~1.5% for 10% Fe concentration and ~6% for 0.5% Fe concentration. The results indicate that Fe has no strong site-preference in NiAl but tends to reside on the site of the stoichiometrically deficient host element.

ACKNOWLEDGMENTS

This research was supported by the Division of Materials Sciences and by the Assistant Secretary for Energy Efficiency and Renewable Energy, Office of Industrial Technologies, Advanced Industrial Materials Program, U.S. Department of Energy, under contract DE-AC05-84OR21400 with Martin Marietta Energy Systems, Inc. and by an appointment (IMA) to the Oak Ridge National Laboratory (ORNL) Postdoctoral Research Associates Program, which is administered jointly by the Oak Ridge Institute for Science and Education (ORISE) and ORNL.

REFERENCES

1. J.D. Cotton, R.D. Noebe, and M.J. Kaufmann, in *Structural Intermetallics*, edited by R. Darolia, J.J. Lewandowski, C.T. Liu, P.L. Martin, D.B. Miracle, and M.V. Nathal (The Minerals, Metals, and Materials Society, 1993), p. 513.
2. M.G. Walls, Microsc. Microanal. Microstruct. **3**, 443 (1992).
3. I.M. Anderson and J. Bentley, in *Electron Microscopy 1994*, Proc. 13th ICEM, (Editions de Physique, Paris, 1994), p. 609; I.M. Anderson, A.J. Duncan, and J. Bentley, ibid., p. 679.
4. J.C.H. Spence and J. Taftø, J. Microsc. **130**, 147 (1983).
5. S.J. Pennycook, Ultramicroscopy **26**, 239 (1988).
6. J. Bentley, in Proc. 44th EMSA (San Francisco Press, San Francisco, CA, 1986), p. 704.
7. P.R. Monroe and I. Baker, J. Mat. Res. **7**, 2119 (1992).
8. C.J. Rossouw, P.S. Turner, T.J. White, and A.J. O'Connor, Phil Mag Lett **60**, 225 (1989).
9. J. Bentley, I.M. Anderson, and E.A. Kenik, Microbeam Analysis **3**, S191 (1994).
10. M.K. Miller and J.A. Horton, Scripta Metall. **20**, 1125 (1986).
11. R.D. Noebe, R.R. Bowman, and M.V. Nathal, Int. Mater. Rev. **38**, 193 (1993).

DISCLAIMER